14th International Beam Instrumentation Conference,Liverpool, UK JACoW Publishing
ISBN: 978-3-95450-262-2 ISSN: 2673-5350 doi: 10.18429/JACoW-IBIC2025-TUPCO03

STATUS OF THE SYNCHROTRON RADIATION TELESCOPE AT THE LARGE HADRON COLLIDER

D. Butti*, E. Bravin, S. Burger, A. Guerrero, F. Roncarolo, G. Trad, CERN, Geneva, Switzerland

Abstract

Accurate and continuous measurement of the transverse beam profile is essential for optimizing machine performance and ensuring beam quality in particle accelerators. At the Large Hadron Collider (LHC), this task is performed non-invasively and in real time by the Synchrotron Radiation Telescope (BSRT).

Operational since 2015, the BSRT has undergone significant consolidation and a series of upgrades, enhancing its reliability and performance. It operates under conditions that pose specific challenges not commonly encountered in synchrotron radiation diagnostics at electron facilities. These include the complexity of the radiation source, consisting of multiple magnetic elements that evolve during the machine cycle, operation near the diffraction limit in the shortwave Ultra Violet (UV), and the requirement for full remote control, as the setup is inaccessible during regular machine operation.

This contribution presents the current status of the BSRT system, reviewing its key capabilities, operational limitations, and its role in both routine machine operations and dedicated beam physics studies. Finally, an outlook is provided on future upgrades currently under study, aimed at extending the instrument's performance and ensuring its readiness for the upcoming High-Luminosity LHC era.

INTRODUCTION

At the Large Hadron Collider (LHC), non-invasive emittance monitoring is performed using beam synchrotron radiation telescopes (BSRTs) [1]. The instrument version installed at the LHC startup was based on the Large Electron-Positron collider (LEP) design [2–4]. While online relative measurements proved valuable during the early stages of machine commissioning [5–7], the overall performance was limited by the complexity of the system, based on reflective optics. Moreover, the synchrotron radiation (SR) extraction system, consisting of a metallic mirror protruding into the beam chamber, suffered severe damage due to beam coupling impedance and related RF heating issues [8]. During the Long Shutdown 2 (2018-2021), the 8-element reflective optics was replaced with a simpler double-lens refractor [9] designed to shift the working wavelength to the shortwave Ultra Violet (UV) in order to push the diffraction limit at high beam energy [10]. The light extraction system was also redesigned to provide a low-impedance solution based on a fully dielectric in-vacuum mirror [11].

Since this major redesign, the BSRT has been continuously upgraded to improve the reliability of both the hardware and the control system.

* daniele.butti@cern.ch

HARDWARE AND CONTROLS

Two SR systems, one per beam, are installed on opposite sides of LHC Point 4, as shown in Fig. 1. The extracted optical SR is used by a variety of operational and R&D diagnostics, both longitudinal and transverse, with the BSRT serving as the main instrument for transverse beam size measurements.

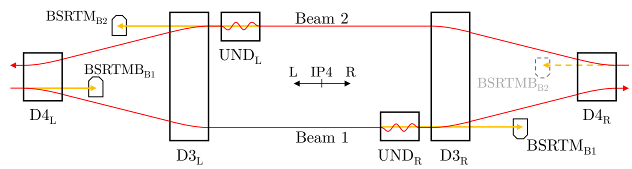

Figure 1: Layout of LHC Point 4 with the operational (BSRTM) and planned (BSRTMB) SR extraction systems.

Since multiple magnetic elements contribute to the emitted radiation, the spatial and spectral characteristics of the light depend significantly on the beam energy [12]. At the injection energy of 450 GeV, superconducting two-period undulators provide visible SR with a spectrum peaking at 600 nm and a spectral width of about 300 nm. As the energy ramp begins, the undulators are turned off, since their spectra drift into the soft X-ray range, which is not used for diagnostics and harmful to the extraction mirror. From 2 TeV, the D3 dipoles become the dominant source of visible SR. The critical wavelength of these dipoles lies in the visible domain at around 3 TeV, and decreases to 60 nm at the flat-top energy of 6.8 TeV, leaving the long-wavelength tail of the broad dipole spectrum in the optical region. SR is intercepted approximately 15 m downstream of the source by an in-vacuum mirror (BSRTM), which deflects it downward and sends it through a viewport into a hutch beneath the beam pipe. The hutch is light-tight and radiation-shielded, allowing the use of off-the-shelf electronics [13]. Inside the hutch, the light is distributed on an optical table to the various SR monitors, as shown in Fig. 2.

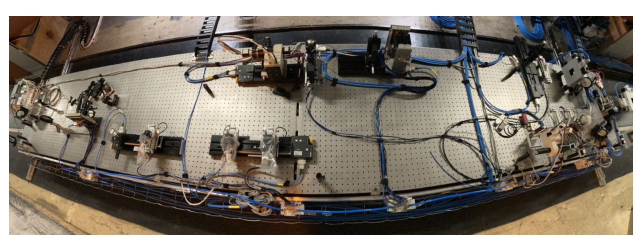

Figure 2: LHC Beam1 SR optical table, before its positioning into the light-tight and radiation-shielded hutch.

The current optical design of the BSRT is based on a Keplerian-type refractor. A main objective lens with f =

ISBN: 978-3-95450-262-2 ISSN: 2673-5350 doi: 10.18429/JACoW-IBIC2025-TUPCO03

4810 mm creates a first real image of the source, which is then re-imaged by a $f = 290$ mm lens to achieve an overall magnification of $M \approx 0.22$.

Two optical configurations are implemented: achromatic lenses optimized for the visible range 400-600 nm, and custom lenses optimized for shortwave UV 225-275 nm. The visible configuration is used at injection energy (450 GeV), with SR from the undulator while the UV lenses provide better performance with dipole radiation at high energy. As the beam energy increases, the SR emission angle narrows. At 6.8 TeV, the light aperture is $\vartheta \approx 200$ µrad, which is smaller than the physical aperture of the optics and therefore the dominant factor limiting resolution. For diffraction-limited imaging of dipole SR, the resolution scales as $\sigma_{\mathrm{res}} \propto \lambda^{2/3}$ [14]. Shifting the working wavelength to the shortwave UV mitigates diffraction and enhances the resolution for the smaller, high-energy beams. A band-pass filter of 250 ±5 nm is inserted to monochromatize the broadband dipole radiation when the UV lenses are used. The BSRT control system automatically manages these configurations by inserting the necessary elements into the optical line. In both configurations, focusing is achieved by adjusting the longitudinal position of the second lens. The detector consists of a digital camera (Basler acA1920-40gm) coupled to an image intensifier unit (Hamamatsu C14245). The image intensifier is used primarily to provide fast gating (20 ns), enabling single bunch measurements, rather than for light amplification.

Since the system is installed inside the machine tunnel, access is limited to only a few occasions per year. Lasers and laboratory lamps are used for initial setup and alignment of the optics, but extensive automation is required to remotely tune the system with the actual SR from the beam. Despite its conceptually simple optical layout, the BSRT includes more than 40 actuators, pneumatic and motorized, to provide the necessary control. The steering of the optical line is monitored with cameras observing targets placed at all pupil and image planes of the system.

Significant effort has also been devoted to ensuring the radiation tolerance of the system. Wherever possible, electronics have been relocated outside the machine tunnel. Commercial electronics were radiation-tested to validate their compatibility with the residual levels inside the shielding (TID ~ 0.5 Gy/year, Φ_{HEH} ~ 1.7×10^9 p/cm^{2}year)[1] and radiation-tolerant electronics were developed for control modules located outside the hutch (TID ~ 12 Gy/year, Φ_{HEH} ~ 8×10^9 p/cm^{2}year). Today, only the minimum number of radiation-sensitive devices, such as the detector and network equipment, remain inside the tunnel within the BSRT shielding.

CALIBRATION

An imaging system can, in principle, provide an absolute measurement of the source size, provided that its resolution and magnification are well characterized. The resolution is fully described by the Point Spread Function (PSF), which represents the system's response to a point-like source. Once the PSF is known, the image of an arbitrary source can be described as the convolution of the source distribution with the PSF. Several attempts were made to obtain absolute measurements from the BSRT by characterizing its PSF with resolution targets or calibrated apertures. However, these procedures never yielded results consistent with beam measurements, mainly because SR has specific spatial–spectral properties that significantly affect the PSF and cannot be exactly reproduced by conventional light sources.

To provide accurate beam size values, the BSRT is calibrated against measurements from the beam wire scanners (BWSs), which are considered as a more reliable reference for absolute beam size [15], but can only operate at low beam intensity. Assuming Gaussian profiles for both the beam distribution and the PSF, the BSRT image spot is also Gaussian, with variance

$$\sigma^2_{\mathrm{BSRT,img}} = M^2\left(\sigma^2_{\mathrm{BSRT,beam}} + \sigma^2_{\mathrm{PSF}}\right), \qquad (1)$$

where M is the magnification, σ_{PSF} the standard deviation of the PSF, and $\sigma_{\mathrm{BSRT,beam}}$ the beam size at the BSRT location. The latter is obtained from the BWS measurement, transported through the lattice using the betatron functions as $\sigma_{\mathrm{BSRT,beam}} = \sigma_{\mathrm{BWS,beam}}\sqrt{\beta_{\mathrm{BSRT}}/\beta_{\mathrm{BWS}}}$.

In a typical BSRT calibration fill, about 10 bunches are injected with beam sizes spanning the operational emittance range of 1-3 µm and keeping the total intensity below the BWS limit of 1.5×10^{12} protons. The BSRT calibration factors M and σ_{PSF} are obtained from a linear regression of $\sigma^2_{\mathrm{BSRT,img}}$ against $\sigma^2_{\mathrm{BSRT,beam}}$, following the model of Eq. (1). Owing to the specific characteristics of the SR source, different calibration factors are found at injection and flat-top energies, as well as between the two transverse beam planes. The system focusing is also determined during the calibration procedure by scanning the longitudinal position of the focusing lens to identify the compromise that minimizes the horizontal and vertical PSFs, at injection and flat-top energies separately.

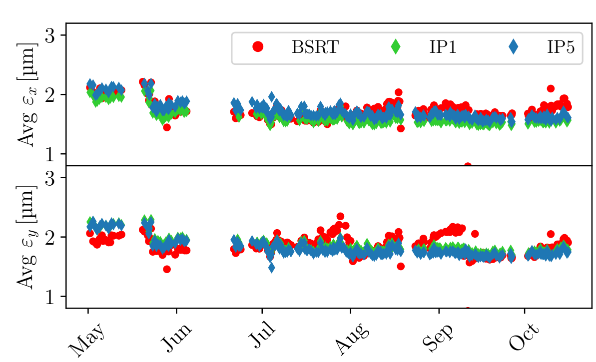

Figure 3: Evolution of the horizontal (top) and vertical (bottom) average emittance during 2024 proton run, as measured by the BSRT and the luminosity scans. Calibration factors were updated on August 1st and September 10th.

[1] Radiation levels expressed as Total Ionizing Dose (TID) and fluence of high-energy hadrons (Φ_{HEH})

14th International Beam Instrumentation Conference,Liverpool, UK JACoW Publishing
ISBN: 978-3-95450-262-2 ISSN: 2673-5350 doi: 10.18429/JACoW-IBIC2025-TUPCO03

Fresh from calibration, the BSRT achieves an accuracy well within the 10 % emittance target required for machine operation [16]. However, the long-term reproducibility of the calibration factors remains a challenge. At injection energy, the accuracy is relatively stable, since beam sizes are on the order of 1 mm, much larger than the typical BSRT resolution of 350 µm. In contrast, calibration stability is critical at flat-top energy, where, even in the shortwave UV, the typical resolution of 200 µm is comparable to beam sizes of about 250 µm. Since the start of LHC Run 3 in 2021, luminosity scans have been regularly performed at the two main Interaction Points (IP1 and IP5) [17], and can be used to probe the stability of the average BSRT emittance measurement. As illustrated in Fig. 3, over long periods the BSRT tends to overestimate the measured beam size, due to the slow degradation of optical components constantly exposed to high-intensity light. Calibration fills take time away from physics production and cannot be performed frequently; nevertheless, calibration factors typically needs to be updated at least twice per year to maintain acceptable accuracy. Calibration drifts affect only the absolute accuracy and do not compromise the quality of relative measurements, which remain stable and reliable.

PERFORMANCE AND LIMITATIONS

The BSRT is routinely used to monitor the quality of the circulating beams. Figure 4 shows an example of the real-time display recorded at the end of machine filling, just before the start of an energy ramp. The instrument reveals a clear horizontal emittance growth as the first injected trains, circulating for longer, appear larger than the most recently injected ones. Thanks to its bunch-by-bunch capability, the BSRT also detects emittance patterns within individual trains, such as vertically blown-up bunches at specific slots, and sporadic horizontal blow-up of a few bunches caused by transverse instabilities.

Besides serving as an emittance monitor, the instrument is also employed in dedicated beam physics studies during Machine Development (MD) periods. Since 2025, BSRT profiles have been successfully used to monitor the content and evolution of the beam-tail population during the injection phase [18, 19], and an online analysis of the beam tails, based on the deconvolution of q-Gaussian functions, has been implemented to extend the simple Gaussian model of Eq. (1), used for standard emittance assessment.

Continuous upgrades of the system have greatly improved its availability. Despite the complexity of the setup, BSRT downtime is limited to only a few events per year, mostly caused by residual radiation effects on the electronics. Such events are promptly detected and recovered thanks to dedicated failure-monitoring and diagnostic tools.

Limitations remain in the instrument performance. The non-reproducibility of the calibration affects the long-term accuracy of absolute measurements at flat-top energy. Measurements taken during the accelerator energy ramp are not reliable, as they are strongly influenced by variations in the

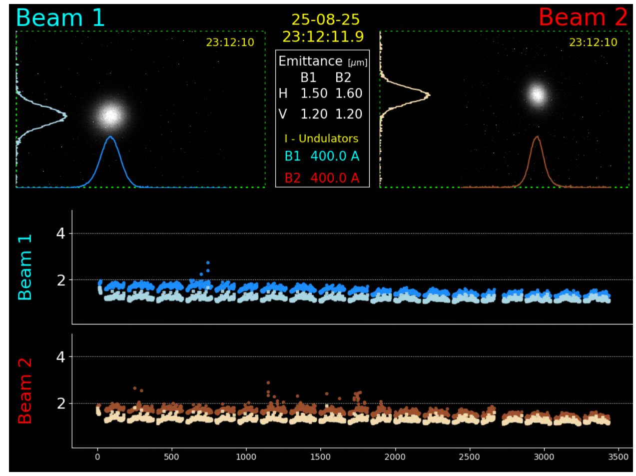

Figure 4: BSRT real-time display. Top: stream of beam images with corresponding profiles and summary of the average beam emittance. Bottom: bunch-by-bunch histograms of horizontal (dark) and vertical (light) emittances.

properties of the SR source. Another limitation arises during ion runs: since the source cannot provide visible SR at 450 GeV, diagnostics at injection are only available for proton beams.

CONCLUSION AND OUTLOOK

The BSRT is today an indispensable tool for beam diagnostics at the LHC, as it remains the only instrument capable of providing continuous, bunch-by-bunch emittance measurements during regular machine operation.

While no major upgrades are planned for the existing instrument, secondary extraction lines (BSRTMB) are under design for the High-Luminosity LHC era [20]. These new lines will extract synchrotron radiation from the D4 magnets and feature a novel extraction mirror that can be inserted closer to the beam, capturing radiation emitted by the core of the dipole. The light will be transported to a service gallery outside the machine tunnel, improving accessibility and suppressing radiation-induced failures. The main application of these secondary lines is to install high-dynamic-range systems for halo monitoring. They will also provide additional emittance diagnostics, offering redundancy to the existing BSRT. The simpler SR source, consisting of a single magnet, will enable reconsideration of alternative optical techniques, such as SR interferometry, previously discarded due to the complexity of the current SR source [12]. These techniques can provide independent measurements to cross-check the imaging results.

In addition to SR-based diagnostics, instrumentation based on beam-gas interactions, such as a Beam-Induced Fluorescence monitor [21] and a Ionization Profile Monitor [22], is being developed. These complementary instruments may help overcome or complement the limitations of the BSRT, to provide richer transverse diagnostics for the future runs of LHC.

ISBN: 978-3-95450-262-2 ISSN: 2673-5350 doi: 10.18429/JACoW-IBIC2025-TUPCO03

REFERENCES

[1] LHC synchrotron radiation monitors online documentation, `https://sr-monitors.docs.cern.ch/`

[2] J. Bosser, C. Bovet, and R. Jung, "Preliminary studies on a profile monitor for the LHC using synchrotron radiation", CERN, Geneva, Switzerland, Rep. CERN-LHC-Note-192, Jun. 1992.

[3] R. Jung *et al.*, "LHC proton beam diagnostics using synchrotron radiation", CERN, Geneva, Switzerland, CERN Yellow Reports: Monographs, 2004. `doi:10.5170/CERN-2004-007`

[4] A. S. Fisher, A. Goldblatt, and T. Lefevre, "The LHC Synchrotron-Light Monitors", in *Proc. DIPAC'09*, Basel, Switzerland, May 2009, paper TUPB03, pp. 164–166.

[5] J. Wenninger, "LHC Beam Diagnostics - the Users Point of View", in *Proc. DIPAC'11*, Hamburg, Germany, May 2011, paper WEOD02, pp. 580–584.

[6] F. Roncarolo *et al.*, "Synchrotron Radiation Measurements at the CERN LHC", in *Proc. DIPAC'11*, Hamburg, Germany, May 2011, paper WEOA04, pp. 550–552.

[7] T. Lefevre *et al.*, "First Beam Measurements with the LHC Synchrotron Light Monitors", in *Proc. IPAC'10*, Kyoto, Japan, May 2010, paper MOPE057, pp. 1104–1106.

[8] F. Roncarolo *et al.*, "Electromagnetic Coupling between High Intensity LHC Beams and the Synchrotron Radiation Monitor Light Extraction System", in *Proc. IPAC'13*, Shanghai, China, May 2013, paper TUPFI063, pp. 1493–1495.

[9] A. Goldblatt, E. Bravin, F. Roncarolo, and G. Trad, "Design and Performance of the Upgraded LHC Synchrotron Light Monitor", in *Proc. IBIC'13*, Oxford, UK, Sep. 2013, paper MOPF08, pp. 220–223.

[10] G. Trad *et al.*, "Performance of the Upgraded Synchrotron Radiation Diagnostics at the LHC", in *Proc. IPAC'16*, Busan, Korea, May 2016, pp. 306–309. `doi:10.18429/JACoW-IPAC2016-MOPMR030`

[11] G. Trad, "Development and optimisation of the SPS and LHC beam diagnostics based on synchrotron radiation monitors", Ph.D. thesis, LSPC, Grenoble, France, May 2015.

[12] D. Butti, "Development of a Synchrotron Radiation Interferometer for Accurate Transverse Beam Size Measurement at the LHC", Ph.D. thesis, Royal Holloway, University of London, UK, May 2024.

[13] K. Tsoulou, V. Vlachoudis, and A. Ferrari, "Simulation of the radiation levels and shielding studies at the BDI positions in IR4", CERN, Geneva, Switzerland, Rep. CERN-LHC-Note-367, May 2005.

[14] K. J. Kim, "Characteristics of synchrotron radiation", *AIP Conf. Proc.*, vol. 184, pp. 565–632, Apr. 1989. `doi:10.1063/1.38046`

[15] J. Emery *et al.*, "The Large Hadron Collider's beam wire scanner consolidation", in *Proc. IBIC'24*, Beijing, China, Sep. 2024, pp. 326–330. `doi:10.18429/JACoW-IBIC2024-WEP29`

[16] R. Tomás, "Beam size measurements requirements for HL-LHC", presented in LHC Beam Size Review, CERN, Geneva, Switzerland, 2019.

[17] M. Hostettler *et al.*, "Luminosity Scans for Beam Diagnostics", *Phys. Rev. Accel. Beams*, vol. 21, p. 102801, 2018. `doi:10.1103/PhysRevAccelBeams.21.102801`

[18] S. Kostoglou, "Emittance evolution in physics and luminosity-calibration fills: what measurements do we have and what did we learn from them?", presented in LumiDays'25, CERN, Geneva, Switzerland, 2025.

[19] M. Rakic *et al.*, "Assessing the origin of the LHC beam halo", presented at the IPAC'25, Taipei, Taiwan, Jun. 2025, paper, THAN1, yet to be published.

[20] D. Butti *et al.*, "Status of the BSRT upgrade for HiLumi", presented in 11th HL-LHC Collaboration Meeting, CERN, Geneva, Switzerland, 2021.

[21] D. Butti *et al.*, "Performance of the Beam Gas Curtain as emittance monitor at the Large Hadron Collider", presented at IBIC'25, Liverpool, UK, September 2025, paper TUPCO04, this conference.

[22] M. McLean *et al.*, "Non-destructive beam profile measurements with an ionisation profile monitor (IPM) based on TimePix3&4 hybrid pixel detectors (HPDs)", in *Proc. IBIC'24*, Beijing, China, Sep. 2024, pp. 289–292. `doi:10.18429/JACoW-IBIC2024-WEP15`